Letter

Holographic batteries

William D. Biggs and Jorge E. Santos
Department of Applied Mathematics and Theoretical Physics, University of Cambridge, Cambridge CB3 0WA, United Kingdom

(Received 28 October 2023; accepted 18 April 2024; published 14 May 2024)

We study a three-dimensional holographic conformal field theory under the influence of a background electric field on a spacetime containing two black hole horizons. The electric background is fixed such that there is potential difference between the two boundary black holes, inducing a conserved current. By constructing the holographic duals to this setup, which are solutions to the Einstein-Maxwell equations with a negative cosmological constant in four dimensions, we calculate, to a fully nonlinear level, the conductivity of the conformal field theory in this background. Interestingly, we find that the conductivity depends nontrivially on the potential difference. The bulk solutions are flowing geometries containing black hole horizons which are non-Killing and have nonzero expansion. We find a novel property that the past boundary of the future horizon lies deep in the bulk and show this property remains present after small perturbations of the temperature difference of the boundary black holes.

DOI: 10.1103/PhysRevD.109.L101904

Introduction. Given a quantum field theory (QFT), a natural avenue of investigation is to test how it behaves under an external electric field. Studying such behavior for a strongly coupled QFT using direct field theory techniques is computationally very challenging (though progress has been made when the system is in the proximity of quantum critical points [1]; see also [2] for a holographic description of a similar setup). However, since its advent, the AdS/CFT correspondence [3–5] has allowed for the indirect study of strongly coupled condensed matter systems via gravitational calculations (see for instance [6] for an excellent review on the topic).

Specifically, we work in the limit of the AdS/CFT duality in which the gravitational theory is well described by classical gravity. In this limit, the duality maps a problem of studying a strongly coupled conformal field theory (CFT) with a large number of degrees of freedom living on a fixed (but possibly curved) background, $\mathcal{B}$, to a gravitational problem in which one must find a corresponding *asymptotically locally anti–de Sitter* (AlAdS) spacetime, called the *bulk*, which possesses a conformal boundary on which the induced metric is conformal to $\mathcal{B}$ (see Ref. [7] for an introduction to this method).

Taking $\mathcal{B}$ to be a black hole background has allowed for the study of Hawking radiation at strong coupling. The dual bulk solutions are generally called *droplets* and *funnels* [8–21], with the distinction between these two classes originating from the structure of the horizons in the bulk. A bulk solution with a horizon connecting two distinct boundary horizons is called a funnel, whereas a bulk solution with horizons each emanating from only a single boundary horizon is called a droplet.

In this Letter, we will focus on four-dimensional global funnels. The boundary geometry will be given by the conformal compactification of the geometry obtained by "patching together" two identical Bañados-Teitelboim-Zanelli (BTZ) black holes (shown on the left in Fig. 1) at infinity. This yields two black holes antipodally situated in the Einstein static universe as sketched in the middle in Fig. 1. There is a well-known solution called the BTZ black string or uniform funnel which connects these two boundary black holes, however, even in the case of vacuum gravity in the bulk, there is a rich structure of bulk solutions beyond this uniform funnel [17–20]. The right-hand sketch in Fig. 1 is a schematic drawing of a global funnel.

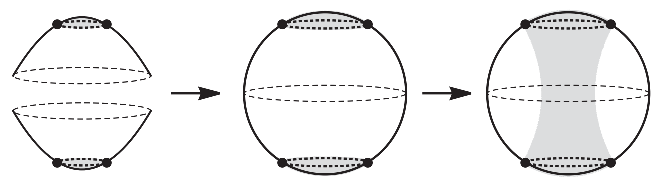

FIG. 1. Some sketches of spatial cross sections of spacetimes of interest. Left: two BTZ black holes with the dashed curves being their asymptomatic boundaries and the dotted line their horizons. The interior is shaded. Middle: the boundary geometry found by patching the BTZ spacetimes together at infinity and then compactifying onto the Einstein static universe. Right: the global funnel, a solution in the bulk with a horizon connecting the two boundary horizons.

We add a chemical potential to the field theory which induces a conserved current, J^μ, and, on the gravitational side of the duality, causes a deformation of the bulk geometry away from the uniform funnel to a new solution to the Einstein-Maxwell equations with a negative cosmological constant. We will define the chemical potential to vary on the boundary background, and in particular fix that it approaches two different values at the two BTZ black hole horizons in the boundary geometry. Since these charged global funnels correspond to the QFT sourced by the two horizons at the same temperature but with a potential difference between them, we dub these solutions as *holographic batteries*.

Calculating the bulk solution allows one to extract the conserved current, J^μ, induced by the source on the field theory side, and so this provides a process to calculate the nonlinear conductivity of the boundary field theory, going beyond the linear regime examined in [22–30]. Interestingly, we find that the conductivity is not a constant value, i.e. the current, J^μ, depends nontrivially on the magnitude of the chemical potential, despite there being no net current, in contrast to what was observed in [31,32].

Moreover, the chemical potential varying across the boundary geometry induces classical flow along the bulk horizon. Unlike previously found solutions containing flowing horizons [16,18,21,33], this flow is not caused by a temperature difference between two asymptotic regions of the bulk horizon, and this means the properties of the holographic batteries are subtly different to these other flowing solutions. In particular, we show that the past boundary of the bulk horizon lies deep in the bulk, as opposed to on one of the points at which the bulk horizon is anchored on the boundary, as seen in all previous flowing black hole geometries. We show that this property is generic by considering holographic batteries in which the boundary black holes can also have a small temperature difference.

Finding the batteries. First let us consider the metric of the BTZ black hole:

$$\mathrm{d}s^2_{\mathrm{BTZ}} = -f(r)\mathrm{d}T^2 + \frac{\mathrm{d}r^2}{f(r)} + r^2\mathrm{d}\varphi^2, \tag{1}$$

with $f(r) = (r^2 - r_0^2)/\ell_3^2$, where r_0 is the radius of the BTZ black hole and ℓ_3 is the three-dimensional AdS length scale. Taking

$$r = \frac{r_0}{x\sqrt{2-x^2}}, \qquad T = \frac{\ell_3^2}{r_0}t, \qquad \varphi = \frac{\ell_3}{r_0}\phi, \tag{2}$$

so that $x = 1$ is the horizon and $x = 0$ is infinity, yields

$$\begin{aligned}\mathrm{d}\tilde{s}^2_{\mathrm{BTZ}} &= \Omega(x)^2\mathrm{d}s^2_{\mathrm{BTZ}},\\ &= \ell_3^2\left[-\mathrm{d}t^2 + \frac{1}{(1-x^2)^2}\left(\frac{4\mathrm{d}x^2}{2-x^2} + \mathrm{d}\phi^2\right)\right],\end{aligned} \tag{3}$$

where we have multiplied the metric by a conformal factor

$$\Omega(x) = \frac{x\sqrt{2-x^2}}{1-x^2}. \tag{4}$$

Note that ϕ has a period of $2\pi r_0/\ell_3$, which we must take into account when calculating any global properties of the solutions. The geometry upon which we wish to study the CFT is obtained by patching two copies of the metric given by $\mathrm{d}\tilde{s}^2_{\mathrm{BTZ}}$ at their boundaries, i.e. at $x = 0$. Thus the boundary metric is given by the metric in (3), with $x \in [-1, 1]$ and $x = \pm 1$ being the two boundary black hole horizons. The temperature of both horizons, measured in units of the original T coordinate, is given by $T_H = r_0/(2\pi\ell_3^2)$.

The idea is to add an electric field on this background which acts as a source and to fix the chemical potential at the two boundary horizons, $x = \pm 1$. Specifically, let us add an electrical source given by the following vector potential:

$$A^{(0)} = \mu g(x)\mathrm{d}t, \tag{5}$$

where $g(x)$ is a profile we are free to choose and which we will design so that $g(1) = +1$ and $g(-1) = -1$. The potential difference between the two horizons is

$$V \coloneqq [A^{(0)} \cdot k]^{x=1}_{x=-1} = 4\pi\mu T_H, \tag{6}$$

where $k = \partial/\partial T$. For the majority of this Letter we take

$$g(x) \coloneqq \sin\left(\frac{\pi}{2}x\sqrt{2-x^2}\right), \tag{7}$$

which we call the *sine profile*.

The ansatz: The addition of an electric source in the boundary theory means that the bulk theory is Einstein-Maxwell with a negative cosmological constant in four dimensions, with the following equations of motion:

$$0 = E_{ab} \coloneqq R_{ab} + \frac{3}{\ell_4^2}g_{ab} - 2T_{ab}, \tag{8a}$$

$$0 = \nabla^a F_{ab}, \tag{8b}$$

where ℓ_4 is the four-dimensional AdS length scale, $F = \mathrm{d}A$ is the field strength tensor of the Maxwell field and the bulk stress tensor is given by

$$T_{ab} = F_a{}^c F_{bc} - \frac{1}{4}g_{ab}F^{cd}F_{cd}. \tag{9}$$

We begin with an *ansatz* in Bondi-Sachs gauge which possesses a null hypersurface at $y = 1$ and a conformal boundary at $y = 0$. We also assume the solutions will be stationary and axisymmetric, with corresponding Killing vector fields ∂_v and ∂_ϕ, respectively. For the gauge field we pick a gauge in which $A_y = 0$. In such a gauge, the *ansatz* is given by

$$\begin{aligned}\mathrm{d}s^2 = \frac{\ell_4^2}{y^2}\Bigg[&q_2^2(-(1-y^2)q_1\mathrm{d}v^2 - 2\mathrm{d}v\mathrm{d}y)\\ &+ \frac{q_5^2}{(1-x^2)^2}\left(\frac{4(\mathrm{d}x-(1-x^2)q_4\mathrm{d}v)^2}{(2-x^2)q_3} + q_3\mathrm{d}\phi^2\right)\Bigg]\end{aligned} \tag{10a}$$

and

$$A = \ell_4\left(q_6 \mathrm{d}v + \frac{q_7}{1-x^2}\mathrm{d}x\right), \tag{10b}$$

where $q_i(x,y)$ are unknown functions which depend upon x and y. Schematically, this spacetime also looks like the right-hand sketch in Fig. 1.

There is still some gauge freedom in the *ansatz* which can be used to fix the radial dependence of either q_2 or q_5 completely. In our case we fix that of q_5, by enforcing

$$q_5(x,y) = 1 + y^2 S_2(x). \tag{11}$$

With such an *ansatz*, the partial differential equations arising from the equations of motion can be solved numerically as a boundary value problem after setting suitable boundary conditions, as was first set out, and more fully explained, in [21] for the case of pure gravity and [34] for Einstein-Maxwell. We have briefly summarized the integration scheme in the Supplemental Material [35]. Let us emphasize here that at the conformal boundary, $y=0$, we set Dirichlet boundary conditions such that the induced metric is conformal to the metric given by (3) and the bulk vector potential is equal, up to a factor of ℓ_4, to the boundary source (5).

We also obtained the solutions using the DeTurck method [36–38], and present the *ansatz* for the solutions in that gauge in the Supplemental Material [35].

Results. The holographic stress tensor, $\langle T_{\mu\nu}\rangle$, and conserved current, $\langle J^\mu\rangle$, can be extracted from the numerical solutions using the standard procedure of holographic renormalization [39], which we describe explicitly in the Supplemental Material [35]. One benefit of the Bondi-Sachs gauge over the DeTurck gauge is that no non-analyticities arise in this procedure.

Conductivity: Of particular interest will be the current, $\langle J^\mu\rangle$, which is conserved:

$$\mathrm{D}_\mu \langle J^\mu\rangle = 0, \tag{12}$$

where D is the covariant derivative associated to the boundary metric, given by (3). We find that

$$\langle J_x\rangle = \frac{\nu C_1}{\ell_3\sqrt{2-x^2}}, \tag{13}$$

where ν is a dimensionless quantity which depends upon the number of degrees of freedom of the CFT and is defined holographically in terms of the dual parameters of the gravitational theory by

$$\nu = \frac{\ell_4^2}{4\pi G_4}, \tag{14}$$

with G_4 being Newton's gravitational constant for the four-dimensional theory. Moreover, as is explained explicitly in the Supplemental Material [35], C_1 is an integration constant that arises from a local analysis of the equations of motion near the conformal boundary. Specifically, one can show that

$$\partial_y q_7(x,0) = (1-x^2)\left(\frac{C_1}{\sqrt{2-x^2}} - \mu g'(x)\right). \tag{15}$$

Though the local analysis of the equations of motion fix that $\partial_y q_7$ must take this functional form near the boundary, one must solve the equations fully, after enforcing regularity deep in the bulk, in order to extract the precise value of C_1.

We can define the *total current*, I, by integrating $\langle J^\mu\rangle$ over a circle, S^1_x, of fixed x at a fixed time slice in the boundary geometry:

$$\begin{aligned} I &\coloneqq \int_{S^1_x} \mathrm{d}\phi \sqrt{g_{\phi\phi}}\, m_\mu \langle J^\mu\rangle, \\ &= 2\nu\pi^2 T_H C_1, \end{aligned} \tag{16}$$

where m^μ unit normal is the unit normal to the circle S^1_x. Let us note again that ϕ has periodicity $2\pi r_0/\ell_3$, which must be taken into account when computing this integral. Note that the value of I is independent of the choice of x at which one fixes the circle, S^1_x, which follows as a direct consequence of (12).

We can describe the *conductance*, G, of the holographic battery by dividing the total current by the potential difference between the two horizons, i.e.

$$G \coloneqq \frac{I}{V} = \frac{\nu\pi C_1}{2\mu}. \tag{17}$$

The conductance depends upon both the choice of profile, $g(x)$, and the magnitude of the chemical potential, μ, or equivalently the potential difference between the two horizons, V. In Fig. 2, we plot the conductance of the holographic batteries, with the sine profile defined by (7), against the potential difference. As $V/T_H \to 0$, the conductance tends to two and it increases with the voltage. Moreover, the gradient of the curve at $V=0$ is zero, meaning that one has to go beyond the linear regime in order to see the nontrivial dependence of the conductance on the potential difference. The derivative of the conductance with respect to V/T_H possesses a turning point, in this case at $V/T_H \simeq 6.62$, with the gradient of the curve decreasing for larger values of V/T_H. It would be of interest to investigate further what happens to G as V/T_H becomes very large, though there are numerical challenges in extending to this region of the parameter space.

The behavior of the conductance appears qualitatively similar for other choices of the profile, $g(x)$, and each satisfy $g(1) = 1 = -g(-1)$. In the Supplemental Material [35] we provide plots of the conductance for other such profiles as well as a proof that $G/\nu \to 2$ as $V/T_H \to 0$ for

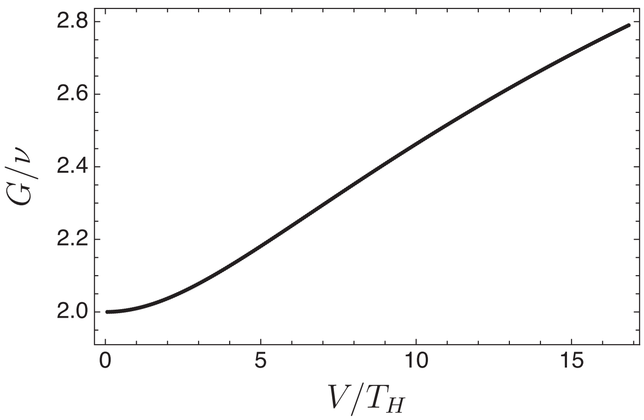

FIG. 2. The conductance of the holographic batteries with the sine profile. Each black dot is a different solution with a different value of the parameter μ. We plot the conductance, G, against the potential difference, V, normalized by the temperature of the black hole horizons, T_H.

any choice of odd profile $g(x)$ by conducting an analysis of the linearized equations of motion.

One can also compute the local *conductivity* of the field by computing the ratio between the x components of the induced current and the source electric field,

$$\sigma(x) \coloneqq \frac{\langle J^x\rangle}{(F^{(0)})^{tx}}, \\ = \frac{2G}{\pi}\cdot\frac{1}{g'(x)\sqrt{2-x^2}}. \tag{18}$$

Since the external electric field is not homogeneous, the conductivity is not constant, however, for a given profile its functional form is always the same, with its magnitude determined by the value of the overall conductance, G.

Energy flow: The addition of a chemical potential causes some heating of the dual CFT by the Joule effect and hence there is flow in the boundary field theory. As was observed in other flowing solutions [16,18,21,33], this means that the bulk horizon is not a Killing horizon. The flow can be expressed via an integral of the holographic stress tensor over a circle, S^1_x, of fixed x in the boundary geometry as follows:

$$\Phi(x) = -\int_{S^1_x} \mathrm{d}\phi \sqrt{-\gamma}\, m_\mu k^\nu \langle T^\mu{}_\nu\rangle, \\ = 2\pi T_H(2G\mu^2 g(x) + 3\pi\nu C_2), \tag{19}$$

where $\gamma_{\mu\nu}$ is the induced metric on a constant x slice of the boundary geometry with determinant γ and unit normal $m_\mu \propto (\mathrm{d}x)_\mu$, whilst $k^\mu \propto (\mathrm{d}t)^\mu$ is the normalized stationary Killing vector field. Note, therefore, that the flow is simply proportional to the $T^x{}_t$ component of the holographic stress tensor, which is given in the Supplemental Material [35]. The constant C_2 is a coefficient in the asymptotic expansion of the q_4 function, which is not fixed by a local analysis of the equations of motion.

In the current case, in which the two boundary horizons have the same temperature and the chemical potential, $g(x)$, is odd, we find empirically, as one would expect, that $C_2 = 0$, and hence there is no net flow between the two horizons. Thus, the flow, $\Phi(x)$, is proportional to the chemical potential, and is odd with $\Phi(x) > 0$ for $x > 0$, meaning that there is flow in both directions originating from the point $x = 0$ and moving outwards towards the boundary. As we will see this behavior near $x = 0$ has an interesting effect on the structure of the horizon of the bulk geometry.

Properties of the bulk horizon: By design, the $y = 1$ is a null hypersurface. We checked explicitly (in a similar manner to in [21]) that there exist future-directed radial null curves from anywhere outside of this hypersurface to the boundary, suggesting it is the event horizon. Let us consider a generator of the horizon, $U_a \propto (\mathrm{d}y)_a$, which can be parametrized by the x coordinate. The affine parameter, $\lambda(x)$, can be obtained from the geodesic equation or from Raychaudhuri's equation.

At the axis of symmetry at $x = 0$, we find that $\lambda'(x) \to 0$, with $\lambda(0)$ taking a finite value, which we are free to choose via an affine transformation as $\lambda(0) = 0$. Moreover, we find that U^a is future directed in both directions moving away from $x = 0$. This suggests that the horizon is better thought of as being generated by two separate future-directed generators, both described by U^a and originating at $x = 0$, one moving in the positive x direction and the other moving in the negative x direction. Hence, the point $x = 0$ is the *past boundary of the future horizon* of the solutions.

Let us restrict to the $x \geq 0$ region of the horizon, since the behavior in the $x \leq 0$ region is similar by symmetry. In the left-hand panel of Fig. 3, we plot the affine parameter along the generator against the x coordinate in a log plot.

Given our affinely parametrized null geodesic U^a, the B tensor is given by $B_{IJ} = \nabla_I U_J$, where I and J run over

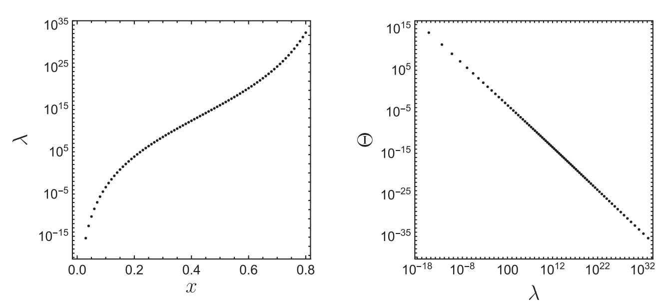

FIG. 3. Left: the affine parameter, λ, along the generator of the $x > 0$ region of the horizon, plotted in a log plot against the coordinate x, for a holographic battery with $\mu = 0.24$. Here we have made the choice that $\lambda(0) = 0$ and $\lambda'(0.1) = 0.1$. Right: the expansion, Θ, along the generator for this holographic battery, plotted in a log-log plot against λ. The expansion diverges at $\lambda = 0$.

$\{v, \phi\}$. The expansion, Θ, and shear, σ_{IJ}, are the trace and symmetric-traceless parts of this tensor, respectively. The fact that $\lambda'(x) \to 0$ as $x \to 0$ means that the expansion and shear diverge as $x \to 0$ along the horizon. In the right-hand panel of Fig. 3 we have plotted the expansion against the affine parameter along the generator of the $x > 0$ region of the horizon.

In flowing horizons, the past boundary is generally situated at the point at which the flow along the horizon emanates from and, moreover, the expansion diverges at this point. In the previous cases [16,18,21], the flow was induced by a temperature difference between the boundary black holes meaning that the past boundary tended to be the hotter boundary horizon. However, in the current case there is no temperature difference; the flow is instead induced by the Joule effect, emerging from $x = 0$ and proceeding outwards, towards the boundary black holes, situated at $x = \pm 1$. Hence, our case is distinct in that the past boundary is situated spatially in the *center* of the horizon with the future-directed horizon generators extending outwards in either direction. This has another interesting consequence: at $x = 0$ (and only at $x = 0$), the generator U^a coincides with the stationary Killing vector, $U^a \propto (\partial_v)^a$, meaning that the Killing vector is a generator of the horizon only on a proper submanifold of the horizon. To our knowledge, this feature has so far not been found to occur in any other instances of flowing horizons.

The divergent expansion at $x = 0$ suggests that the tidal forces between neighboring horizon generators diverges at this point. However, since the future-directed generators emerge from this point, this singularity is always in their far past. If we instead consider the geodesics of infalling observers, then we find no infinite tidal forces are felt for such neighboring geodesics, even near $x = 0$, hence these solutions do not contain any physical singularities.

Detuning the temperatures: One may wonder whether this property of the past boundary of the future horizon of the holographic batteries lying deep in the bulk is generic or simply a product of the symmetry of the setup. To investigate this, we detune the temperatures by adding a nontrivial profile to the g_{tt} component of the boundary geometry:

$$ds^2_{\text{detuned}} = -\ell_3^2 h(x)^2 dt^2 + \frac{\ell_3^2}{(1-x^2)^2}\left(\frac{4dx^2}{2-x^2} + d\phi^2\right), \quad (20a)$$

where

$$h(x) := 1 + \beta \sin\left(\frac{\pi}{2} x \sqrt{2 - x^2}\right), \quad (20b)$$

so that the ratio between the temperatures of the two boundary horizons is $(1 + \beta)/(1 - \beta)$. The *detuned holographic batteries* are the bulk duals to the CFT on this background, still under the influence of an additional chemical potential, given by (7). The method to find the detuned solutions is almost identical to the previous, tuned case, with the *ansatz* only slightly modified to accommodate for the nontrivial $h(x)$ profile. Note, one can recover the tuned holographic batteries by taking $\beta = 0$.

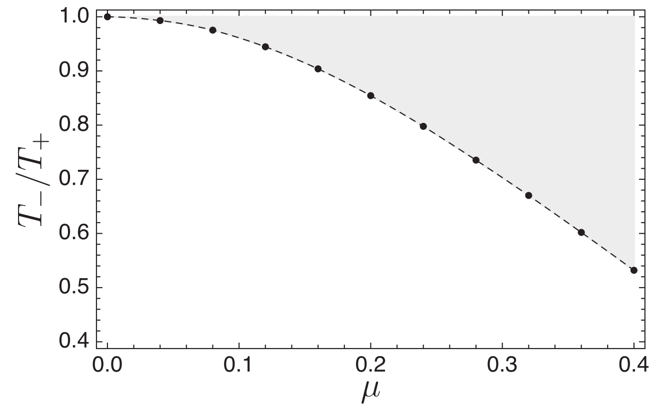

FIG. 4. The region in the parameter space of the detuned holographic batteries in which the past boundary of the horizon lies in the bulk rather than being anchored on the conformal boundary at the hotter boundary black hole. The chemical potential is fixed to be $\pm\mu$ on the horizon with temperature $T_\pm$, respectively, where without loss of generality $T_+ > T_-$.

Interestingly, we find that there is an open set in the parameter space, depicted by the shaded region in Fig. 4, in which the flow vanishes at some point along the horizon and hence the past boundary of the future horizon lies deep in the bulk. Roughly speaking, for these solutions, the contribution to the flow from the temperature difference is not large enough to everywhere overcome the flow due to the Joule effect and cause the flow to be in the same direction throughout the boundary geometry.

Discussion of dominance: Finally, one may wonder whether the charged funnels dominate over a solution with the same boundary geometry in which two droplets emerge from the boundary horizons but do not connect in the bulk, though it is yet to be explicitly shown that such a solution exists for $\mu \neq 0$. Due to the fact the funnels are flowing solutions, there will be difficulty in using thermodynamic arguments since the free energy is not well defined (a problem also faced in [21]). However, it is known that the uniform funnel dominates for a BTZ black hole with a large enough radius [10], and physically one would expect that by adding a charge difference between the two boundary black holes one would remain in the phase in which the funnel dominates.

Acknowledgments. We would like to thank Sean Hartnoll, Gary Horowitz, and Don Marolf for reading an earlier version of this paper and for providing critical comments. We would also like to thank Sean Hartnoll for drawing our attention to Ref. [1]. W. B. was supported by an STFC studentship, Grant No. ST/S505298/1, and a Vice

Chancellor's award from the University of Cambridge, and J. E. S. has been partially supported by STFC consolidated Grant No. ST/T000694/1. The numerical component of this study was carried out using the computational facilities of the Fawcett High Performance Computing system at the Faculty of Mathematics, University of Cambridge, funded by STFC consolidated Grants No. ST/P000681/1, No. ST/T000694/1, and No. ST/P000673/1.

[1] A. G. Green and S. L. Sondhi, Nonlinear quantum critical transport and the schwinger mechanism for a superfluid-mott-insulator transition of bosons, Phys. Rev. Lett. **95**, 267001 (2005).
[2] J. Sonner and A. G. Green, Hawking radiation and non-equilibrium quantum critical current noise, Phys. Rev. Lett. **109**, 091601 (2012).
[3] J. Maldacena, The large N limit of superconformal field theories and supergravity, Adv. Theor. Math. Phys. **2**, 231 (1998).
[4] E. Witten, Anti-de Sitter space and holography, Adv. Theor. Math. Phys. **2**, 253 (1998).
[5] O. Aharony, S. S. Gubser, J. Maldacena, H. Ooguri, and Y. Oz, Large N field theories, string theory and gravity, Phys. Rep. **323**, 183 (2000).
[6] S. A. Hartnoll, A. Lucas, and S. Sachdev, *Holographic Quantum Matter* (MIT Press, Cambridge, MA, 2018).
[7] D. Marolf, M. Rangamani, and T. Wiseman, Holographic thermal field theory on curved spacetimes, Classical Quantum Gravity **31**, 063001 (2014).
[8] V. E. Hubeny, D. Marolf, and M. Rangamani, Hawking radiation in large N strongly-coupled field theories, Classical Quantum Gravity **27**, 095015 (2010).
[9] V. E. Hubeny, D. Marolf, and M. Rangamani, Black funnels and droplets from the AdS C-metrics, Classical Quantum Gravity **27**, 025001 (2010).
[10] V. E. Hubeny, D. Marolf, and M. Rangamani, Hawking radiation from AdS black holes, Classical Quantum Gravity **27**, 095018 (2010).
[11] M. M. Caldarelli, O. J. C. Dias, R. Monteiro, and J. E. Santos, Black funnels and droplets in thermal equilibrium, J. High Energy Phys. 05 (2011) 116.
[12] P. Figueras, J. Lucietti, and T. Wiseman, Ricci solitons, Ricci flow, and strongly coupled CFT in the Schwarzschild Unruh or Boulware vacua, Classical Quantum Gravity **28**, 215018 (2011).
[13] J. E. Santos and B. Way, Black funnels, J. High Energy Phys. 12 (2012) 060.
[14] J. E. Santos and B. Way, Black droplets, J. High Energy Phys. 08 (2014) 072.
[15] S. Fischetti, J. E. Santos, and B. Way, Dissonant black droplets and black funnels, Classical Quantum Gravity **34**, 155001 (2017).
[16] J. E. Santos, To go or not to go with the flow: Hawking radiation at strong coupling, J. High Energy Phys. 06 (2020) 104.
[17] S. Fischetti and D. Marolf, Flowing funnels: Heat sources for field theories and the AdS_3 dual of CFT_2 Hawking radiation, Classical Quantum Gravity **29**, 105004 (2012).
[18] S. Fischetti, D. Marolf, and J. E. Santos, AdS flowing black funnels: Stationary AdS black holes with non-Killing horizons and heat transport in the dual CFT, Classical Quantum Gravity **30**, 075001 (2013).
[19] D. Marolf and J. E. Santos, Phases of holographic Hawking radiation on spatially compact spacetimes, J. High Energy Phys. 10 (2019) 250.
[20] R. Emparan, D. Licht, R. Suzuki, M. Tomašević, and B. Way, Black tsunamis and naked singularities in AdS, J. High Energy Phys. 02 (2022) 090.
[21] W. D. Biggs and J. E. Santos, Black tunnels and hammocks, J. High Energy Phys. 11 (2022) 021.
[22] G. T. Horowitz, J. E. Santos, and D. Tong, Optical conductivity with holographic lattices, J. High Energy Phys. 07 (2012) 168.
[23] G. T. Horowitz, J. E. Santos, and D. Tong, Further evidence for lattice-induced scaling, J. High Energy Phys. 11 (2012) 102.
[24] M. Blake, D. Tong, and D. Vegh, Holographic lattices give the graviton an effective mass, Phys. Rev. Lett. **112**, 071602 (2014).
[25] T. Andrade and B. Withers, A simple holographic model of momentum relaxation, J. High Energy Phys. 05 (2014) 101.
[26] A. Donos and J. P. Gauntlett, Holographic Q-lattices, J. High Energy Phys. 04 (2014) 040.
[27] A. Donos and J. P. Gauntlett, Thermoelectric DC conductivities from black hole horizons, J. High Energy Phys. 11 (2014) 081.
[28] A. Donos and J. P. Gauntlett, The thermoelectric properties of inhomogeneous holographic lattices, J. High Energy Phys. 01 (2015) 035.
[29] M. Rangamani, M. Rozali, and D. Smyth, Spatial modulation and conductivities in effective holographic theories, J. High Energy Phys. 07 (2015) 024.
[30] R. A. Davison and B. Goutéraux, Dissecting holographic conductivities, J. High Energy Phys. 09 (2015) 090.
[31] G. T. Horowitz, N. Iqbal, and J. E. Santos, Simple holographic model of nonlinear conductivity, Phys. Rev. D **88**, 126002 (2013).
[32] B. Withers, Nonlinear conductivity and the ringdown of currents in metallic holography, J. High Energy Phys. 10 (2016) 008.
[33] P. Figueras and T. Wiseman, Stationary holographic plasma quenches and numerical methods for non-Killing horizons, Phys. Rev. Lett. **110**, 171602 (2013).
[34] G. T. Horowitz, M. Kolanowski, and J. E. Santos, Almost all extremal black holes in AdS are singular, J. High Energy Phys. 01 (2023) 162.

[35] See the Supplemental Material at http://link.aps.org/supplemental/10.1103/PhysRevD.109.L101904 for a full description of the numerical method, convergence tests and a proof of the universality of the value of the conductance at zero potential difference.

[36] M. Headrick, S. Kitchen, and T. Wiseman, A new approach to static numerical relativity, and its application to Kaluza-Klein black holes, Classical Quantum Gravity **27**, 035002 (2010).

[37] T. Wiseman, Numerical construction of static and stationary black holes, arXiv:1107.5513.

[38] O. J. C. Dias, J. E. Santos, and B. Way, Numerical methods for finding stationary gravitational solutions, Classical Quantum Gravity **33**, 133001 (2016).

[39] S. de Haro, S. N. Solodukhin, and K. Skenderis, Holographic reconstruction of space-time and renormalization in the AdS/CFT correspondence, Commun. Math. Phys. **217**, 595 (2001).